New Light on Allostery: Dynamic Resonance Raman Spectroscopy of Hemoglobin Kempsey†

Xuehua Hu, Kenton R. Rodgers, Ishita Mukerji, and Thomas G. Spiro*

Department of Chemistry, Princeton University, Princeton, New Jersey 08544

Received October 21, 1998; Revised Manuscript Received January 26, 1999

ABSTRACT: On the basis of static and time-resolved resonance Raman spectroscopy of Hb_A and of a mutant, Hb_K (Dα99N), a specific reaction coordinate is proposed for the allosteric transition in human hemoglobin. The heme is held between proximal (F) and distal (E) helices, whose orientation is responsive to forces generated by ligation and deligation. The E and F helices are in turn tethered via H-bonds to the A and H helices. These outer helices follow the E−F motion, thereby repositioning the N- and C-termini, which form the intersubunit salt bridges in the T quaternary structure. When the T state interface is weakened by Asp → Asn substitution at a quaternary H-bond (Hb_K), the Fe−His bond is relaxed and becomes responsive to allosteric effectors. The same E−F motion is observed in Hb_K, but the A−H following motion is delayed, relative to Hb_A, as is the Asn H-bond formation.

Mechanisms of allostery remain outstanding issues in structural biology. Although the limiting structures defining an allosteric transition have been determined for several proteins (*1*), in no case do we know the pathway by which the transition actually occurs. However, there are good prospects for tracing the path in hemoglobin (Hb), which offers a paradigm of protein allostery. The lessons learned from Hb may help establish general principles of allosteric mechanisms.

Numerous Hb crystal structures have established two arrangements for the $\alpha_2\beta_2$ tetramer, one for tetramers which are ligated and the other for tetramers which are unligated. It is well accepted that these quaternary structures are associated with the high- and low-affinity end states of the allosteric transition, R and T (*2, 3*). The R−T transition can be studied in solution via photolysis of the CO adduct, which occurs on the femtosecond time scale (*4, 5*). Subsequent relaxation of the photodissociated molecules from the R to the T states can be monitored spectroscopically. Careful measurement of the heme absorption (*6*) has revealed three protein relaxations, well separated in time, at ∼0.05, ∼0.5, and ∼20 ms. The same time constants were obtained (*7*) by time-resolved ultraviolet resonance Raman (UVRR) spectroscopy, which is sensitive to the environments of tyrosine and tryptophan residues (*8, 9*). Thus there are discrete protein intermediates between the R and T states, which result in common relaxation times for the heme and for the aromatic residues.

Can these intermediates define a structural path for the allosteric transition? To gain further insight into this question, we have examined the mutant Hb Kempsey (Hb_K), in which the Aspβ99 residue is replaced by asparagine. This substitution weakens a critical intersubunit H-bond in the T state and greatly perturbs the protein function (*10, 11*). This weakening is readily detected in the UVRR spectra, but we find that the tetramer does not revert to the R state in the absence of ligand. Moreover the time course of the R → T transition is essentially unaltered, except for a detectable lag in the formation of the final T state contacts. A specific model of the allosteric transition can be constructed on the basis of these findings (Figure 1).

EXPERIMENTAL PROCEDURES

Fresh human blood containing Hb_K was supplied by Dr. Bunn at Harvard Medical School, and Hb_K was separated from Hb_A as previously described (*10*). The static UVRR experiments were carried out as previously (*12*), and deoxy-Hb_K was generated by photolysis of Hb_KCO with continuous white light illumination at 4 °C under nitrogen. The apparatus and procedures for time-resolved UVRR experiments were as described before (*13*). Solutions used in the UVRR experiments contained twice recrystallized 0.2 M $NaClO_4$ as an internal intensity standard. Visible resonance Raman spectroscopy was performed using the 441.6 nm line from a continuous wave helium−cadmium laser, as reported elsewhere (*14*).

RESULTS AND DISCUSSION

Weakened T State Contacts upon Aspβ99/Asn Substitution. The Hb_K mutation merely involves an isosteric substitution of carboxylate by carboxamide at Aspβ99 (Figure 2), but it has profound functional consequences. The oxygen affinity is raised, while cooperativity and the Bohr effect are greatly diminished (*10, 11*). Also, the dimer/tetramer assembly free energy is lowered, from −14.3 kcal/mol in deoxyHb_A to −8.4 kcal/mol in deoxyHb_K (*15*). All of these changes are consistent with destabilization of the T state relative to the R state, as a result of the weakened H-bond with Tyrα42.

UVRR difference spectra between deoxyHb_K and Hb_K-CO (Figure 3) reveal that the T state contacts are indeed

† This work was supported by NIH Grant GM25158 from the National Institute of General Medical Sciences.

* To whom correspondence should be addressed.

10.1021/bi982513c CCC: $18.00
Published on Web 03/03/1999

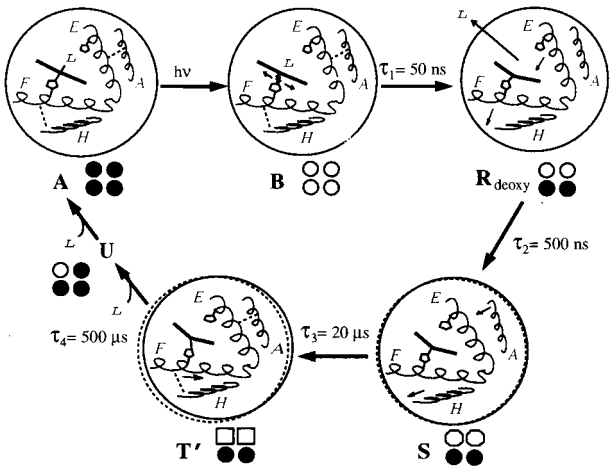

FIGURE 1: Model for the allosteric reaction coordinate of Hb_A, initiated by CO (represented by L) photolysis. The average ligation state of the tetramers is indicated by filled (ligated) and empty (deligated) symbols, circles for the R quaternary structure, squares for the T quaternary structure, and octagons for the S intermediate, which is between R and T. The EF clamshell and the terminal A and H helices are shown for one of the subunits, which loses CO in R_{deoxy}. Photolysis of HbCO (A) produces the geminate intermediate B, in which the Fe−CO bond is broken and strain is stored in the Fe−N (porphyrin and His) bonds prior to large-scale protein motion. These forces generate a rotation of the EF clamshell, which impels the CO either to rebind or to depart the heme pocket, breaking the H-bond tethers between the A and E helices and the F and H helices (R_{deoxy} intermediate). The A and H helices follow, to re-form the H-bonds, thereby loosening the R state quaternary contacts and positioning the C- and N-termini for salt-bridge formation (S intermediate). These contacts lock into place in the T′ intermediate and force lateral motion of the F helix, straining the Fe−His bond. Recombination of one CO from solution produces the triligated intermediate U, which has the R_{deoxy} structure, and the final CO recombination completes the cycle.

weakened, but they are not broken. The spectra contain the same features seen for Hb_A, at about one-half the intensity. These features arise primarily from the Trpβ37···Aspα94 and Tyrα42···Asp(Asn)β99 H-bonds at the $\alpha_1\beta_2$ interface (*2*), which are present in the T but not in the R quaternary structure (Figure 2). The Trpβ37 intensity is augmented by the H-bond-induced red shift of the excitation profile, while the Tyrα42 interaction is manifested as an upshift in the Y8a/8b mode frequencies, which produces the sigmoidal Y8a/8b signals in the difference spectra (*13*). The weakened difference signals in Hb_K imply weakening of both quaternary contacts.

The Y8a/8b upshift is not due to the H-bond donation from Tyrα42, which would ordinarily produce a downshift (*8*), but rather to compensating polarization via H-bond acceptance from the backbone NH of Aspα94, and particularly via the positive charge of the Argα40 side chain (Figure 2), which moves closer to the Tyrα42 side chain in the T structure (*16*). We measured the Y8a upshift to be ~1.6 cm^{-1} in normal hemoglobin (Hb_A) (*13*), but ~0.8 cm^{-1} in Hb_K; thus the compensating polarization is cut in half by the replacement of the negatively charged Aspβ99 carboxylate with a neutral carboxamide. Electrostatics can also explain the weakening of the Trpβ37···Aspα94 H-bond, because the carboxylate side chains of Aspα94 and Aspβ99 are only 5 Å apart (Figure 2). Their mutual repulsion must be a factor in maintaining correct orientation for the quaternary H-bonds, and this repulsion is eliminated by the carboxamide replacement. It seems likely that charge neutralization is a major factor in destabilizing the entire $\alpha_1\beta_2$ interface in deoxyHb_K.

However, this destabilization does not produce a switch to the R quaternary structure. If it did, the UVRR difference spectrum would show a characteristic set of negative tryptophan and tyrosine bands, called the R_{deoxy} spectrum (*17*). This spectrum is seen when the deoxyHb_A is destabilized by chemical removal of the α chain C-terminal residues, Argα141 (Figure 3). In that construct, raising the pH to 9 lowers the T state stability enough to switch the structure to the R (*18*). But this does not happen for deoxyHb_K.

Indeed, the UVRR difference spectra are affected very little by solution conditions (Figure 3). Even when the deoxyHb_K is stabilized by lowering the pH to 6.5 and adding the allosteric effector IHP (inositol hexaphosphate), the UVRR difference bands are intensified only slightly. This behavior is consistent with the greatly diminished Bohr effect in Hb_K (*10, 11*). The main Bohr residues (*2, 19*) are at the β chain C-terminus, Hisβ146, and at the α chain N-terminus, Valα1. These residues form salt bridges at either edge of the $\alpha_1\beta_2$ interface in the T but not the R state, resulting in elevated T state pK_a's (*19*). We infer that weakening of the Hb_K salt bridges is coupled to weakening of the other $\alpha_1\beta_2$ contacts, thereby reducing the pK_a changes and the Bohr effect. Conversely, the T contacts are strengthened to only a limited extent by proton or effector binding, as seen in the UVRR difference spectra.

The R_{deoxy} Structure: Rotation of the EF Clamshell. The UVRR spectrum of fully ligated Hb is independent of the nature of the ligand. Thus difference spectra between HbCO, HbO_2 or Hb^+CN^-, Hb^+F^- are at baseline, provided the tetramers are fully ligated (*14, 20*). Likewise, only noise is observed when the spectra of Hb_ACO and Hb_KCO are subtracted from each other (data not shown). The R structure is unaffected by the Hb_K mutation, since the Aspβ99 side chain is partially exposed to solvent in the R structure (*2, 13*).

However, whenever this invariant tetraligated spectrum is subtracted from the spectrum of R state tetramers having one or more unligated subunits, the distinctive R_{deoxy} difference spectrum is observed (see, e.g., desArgα141 at pH 9—Figure 3). This is also the spectrum of the 0.05 μs photointermediate of Hb_ACO (Figure 1) (*7*). Hb_KCO likewise yields the R_{deoxy} spectrum 0.03 μs after photolysis (Figure 4). Thus the structure change signaled by the R_{deoxy} spectrum is part of the allosteric pathway. Moreover, the R_{deoxy} spectrum reappears (*7*) for the U intermediate (Figure 1), which results from second-order recombination of CO with the diligated T′ intermediate (see below). With three ligands, the U intermediate returns to the R state, but still has an unligated subunit.

We attribute this spectrum to a characteristic motion of the E and F helices, which are distal and proximal to the heme (Figure 2). When the Fe−CO bond is broken, the heme is converted to a high-spin state, in which the Fe−N bonds are lengthened and the Fe is displaced from the heme plane toward the proximal histidine (*21*). Since the proximal histidine residue is part of the F helix, the result of this stereochemical change is motion of the F helix away from the heme. On the distal side, escape of the CO from the heme pocket relieves its steric interactions with distal residues, allowing the E helix to move toward the heme. The E and

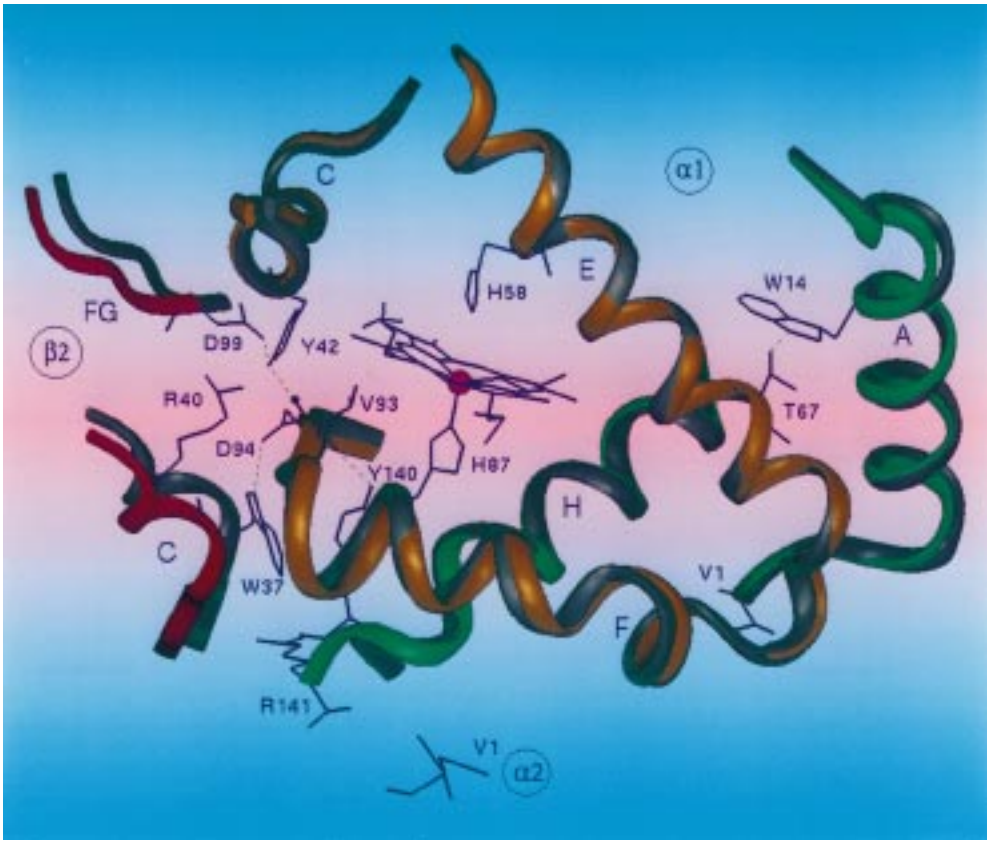

FIGURE 2: Helix representation of the α chains and the $\alpha_1\beta_2$ interface of oxyHb$_A$ (PDB 1HHO) colored gray, and of deoxyHb (PDB 2HHB) (*35, 36*) colored brown, green, and red, with the α chains superimposed. Critical side chains are shown in their deoxyHb positions. The tertiary H-bonds which are present in both R and T states, but broken in the R_{deoxy} intermediate, are Trpα14···Thrα67 and Tyrα140···Valα93 (Trpβ15···Serβ72 and Tyrβ145···Valβ98 in the β chains). The T state quaternary H-bonds, Trpβ37···Aspα94 and Tyrα42···Aspβ99 (reinforced by polarization from Argα40 guanidium and the Aspα94 NH), are broken in the R state. Shown at the bottom of the figure is the α_2 N-terminal Valα1 which forms a salt bridge with α_1 C-terminal Argα141 in the T state.

F helices form a "clamshell" around the heme, hinged at the EF corner (Figure 2). The combined E and F helix motion produces a partial rotation of the clamshell, relative to the heme (Figure 1).

However, the E and F helices are tethered to the outer helices, A and H, by H-bonds (Figure 2). The E−A tether is the H-bond between the A helix residues Trpα14/β15 and the OH groups of the E helix residues Thrα67/Serβ72, whereas the F−H tether is the H-bond between the H helix residues Tyrα140/β145 and the backbone carbonyl groups of the F helix residues Valα93/β98. The R_{deoxy} difference spectrum arises from the weakening of these tethers as a result of the clamshell rotation. When the H-bonds are weakened, the excitation profiles are blue-shifted (*13*), resulting in loss of RR intensity and negative bands in the R_{deoxy} difference spectrum for the H-bond donor tryptophan and tyrosine residues.

This interpretation is strongly supported by the W3 difference band, which is at the position of the interior residues, Trpα14 and β15, not the position of the interface residue Trpβ37. As confirmed by mutation and isotope substitution (*12, 13*), the latter is ∼10 cm^{-1} lower (see inset, Figure 3) because of the dependence of W3 on the dihedral angle about the bond between the indole ring and the C_β atom (*7, 9*). Trpβ37 does not contribute to the R_{deoxy} difference spectrum, consistent with the absence of motion at the subunit interfaces. Only the clamshell moves in response to deligation within the R state.

The tyrosine band assignments are less certain, because there are six tyrosine residues per dimer, and significant dispersion of their positions has not been detected. However, Tyrα42 is unlikely to be responsible for the early negative signals, since its H-bond is formed only in the later stages of the allosteric transition (see below); thus it is plausible that the R_{deoxy} tyrosine bands arise from H-bond weakening of the penultimate tyrosine residues, which form the F−H helix tethers. Moreover, this assignment is strongly supported by site-directed mutagenesis. When Tyrβ145 is replaced by phenylalanine, the binding energetics are essentially unaffected, but the rate of the R → T transition is substantially retarded (*22*). This is just what would be expected if the Tyrβ145 H-bond is lost in a fast initial transient and re-formed in a subsequent slower transient (see next section).

Upon laser photolysis of HbCO, the Fe−CO bond breaks in femtoseconds (*4, 5*), but the CO remains next to the heme for some time, as suggested by its behavior in carboxymyoglobin (*5, 23*). In this geminate, or B state (*24*), the heme is expanded (*21*) and the bond from the Fe to the proximal histidine is compressed [230 cm^{-1} stretching frequency (*7, 25*)], indicating resistance to the displacement of the Fe from the heme plane (Figure 1). About 50% of the CO recombines geminately, with a time constant of 0.05 μs, the same as the time constant for development of the R_{deoxy} signal and for the relaxation of the heme expansion and the Fe−His bond compression (see Figure 1 for the kinetic scheme) (*7*). We propose that this is the time constant for the clamshell

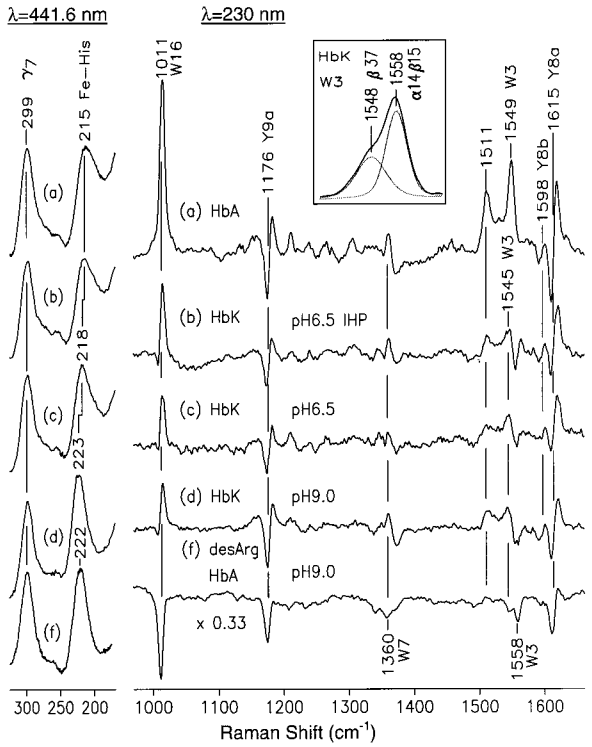

FIGURE 3: Fe−His band region of the Soret-excited RR spectra (left panel) and UVRR difference spectra (relative to HbCO, right panel) of the indicated deoxyHb solutions. The inset is the parent Hb_K W3 band UVRR envelope, showing the frequency separation between Trpβ37 (1548 cm^{-1} shoulder) and Trpα14 and -β15 (1558 cm^{-1} main peak). Trpβ37 makes a positive contribution to T state difference spectra, reflecting formation of the quaternary Trpβ37··· Aspα94 H-bond, while Trpα14 and -β15 make a negative contribution to R_{deoxy} difference spectra, reflecting loss of their tertiary H-bonds. Hb_K at pH 6.5 and in the presence of IHP has the same downshifted Fe−His RR band as Hb_A (top), but the UVRR difference features are only half as strong. Hb_K at pH 9 has the same Fe−His band as desArgα141 Hb (bottom; reproduced from ref *18*), but the UVRR difference bands are nearly unaltered, whereas desArgα141 Hb is in the R state, as revealed by the strong (see 0.33 scale factor) R_{deoxy} difference bands. Hb concentrations were 0.25 mM in 20 mM Bis-Tris buffer (pH 6.5) and 20 mM borate buffer (pH 9).

rotation, which moves the F helix away, relaxing the heme, and moves the E helix toward the heme, forcing the CO either to rebind or to escape from the heme pocket. [The chain specificity of the geminate recombination is unknown. A random distribution is unlikely since it would produce a significant population of triligated tetramers, which would retain the R_{deoxy} signature until recombined with CO from solution. But the R_{deoxy} spectrum disappears entirely in 0.5 μs for Hb_A (*7*) (see next section). It therefore seems likely that geminate recombination is specific to the α or the β chains, or else to a single $\alpha\beta$ dimer.]

The weakening of the interhelical H-bonds represents an energy cost of the clamshell rotation. It is paid for by the relief of nonbonded forces from the expanded heme and the dissociated CO. The extra energy is regained when the CO rebinds, reversing the clamshell rotation. This may be the origin of quaternary enhancement (*26*), which refers to the fact that the free energy associated with the binding of the fourth ligand is greater than the ligation free energy of (noncooperative) dimers. We infer that the clamshell rotation only costs energy within the confines of the R state tetramer, which restrains motion of the outer A and H helices.

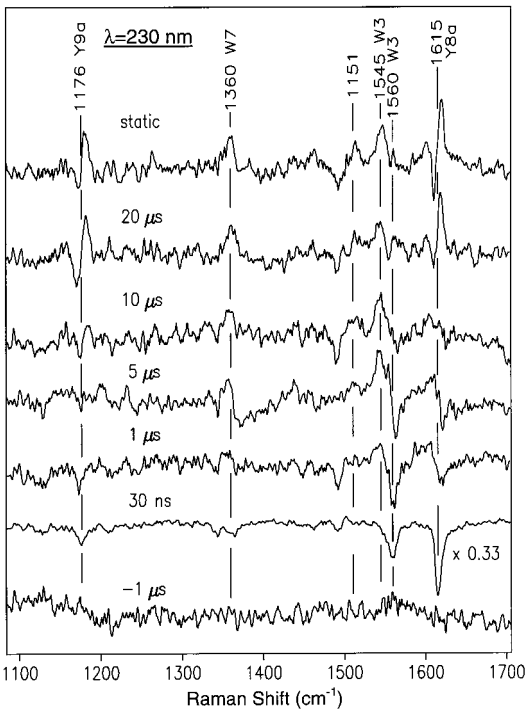

FIGURE 4: Time-resolved UVRR difference spectra of Hb_KCO (0.25 mM in 10 mM phosphate buffer at pH 7) at the indicated delays after a 419 nm photolyzing pulse. As with Hb_A (*7*), a strong R_{deoxy} difference spectrum is seen at early times and later this dies away and is replaced by a spectrum closely resembling the static deoxyHb_K minus Hb_KCO difference spectrum (top). However, the development of the final tyrosine signals (Y8a, Y9a) as well as the loss of the R_{deoxy} signals is delayed relative to the tryptophan signals (W3, W7), whereas they are synchronous in Hb_A. The −1 μs control spectrum (bottom) shows the level of subtraction artifacts.

S Intermediate and Quaternary Motion. In the 0.5 μs transient of Hb_A the R_{deoxy} difference spectrum disappears completely and is replaced by a difference UVRR spectrum with very weak features, which are at the same positions as the static T-minus-R difference spectrum (*7*). These weak features suggest that the final T contacts are formed incipiently in the S intermediate (Figure 1). Moreover, the loss of the R_{deoxy} spectrum implies restoration of the E−A and F−H interhelical H-bonds (Figure 2). We propose that the clamshell reorientation in the R_{deoxy} intermediate induces a following motion of the A and H helices, driven by recovery of the interhelical H-bonds (Figure 1). The A and H helices are not hinged, like the EF clamshell, but they are joined by a set of H-bonds (*18*) and are thus constrained to move in concert with each other. This following motion repositions the N- and C-termini, which are at the ends of the A and H helices.

The N- and C-termini are critical elements of the T quaternary structure, since they form salt bridges, which are broken in the R structure (*2*). Thus their repositioning in the S intermediate is a necessary prelude to the formation of the T state contacts. We envision the S intermediate as one in which the interdimer interface is dynamic. The R state interface contacts have been broken by the helix motions after deligation, and the interfacial residues are being positioned to dock with their T state partners. The Fe−His bond remains relaxed [222 cm^{-1} stretching frequency (*7*)].

The limited time-resolved UVRR data for Hb_K preclude detailed kinetic analysis as was carried out for Hb_A.

Qualitatively the time course is similar, but there is a noticeable delay in the decay of the R_{deoxy} signal (Figure 4). Negative tryptophan and tyrosine bands can still be seen at 1 and 5 μs for Hb_K, but are absent in the 1 μs spectrum of Hb_A (*7*). Thus the movement of the A and H helices appears to be slowed in Hb_K, by a factor of ~10.

The T′ Intermediate: Applying Tension. In the 20 μs phase (Figure 1), the UVRR difference spectrum of Hb_A develops the same bands as are seen in the static T-minus-R difference spectrum (*7*) (Figure 3). [However, the intensities are only half the static intensities, as a result of T′ being diligated. This halving of the intensity is reproduced in cyanometHb hybrids when two ligands are in a single $\alpha\beta$ dimer (*17*), but when they are in opposite dimers, a mixture of T and R_{deoxy} signal is produced (*14*). The T′ state is inferred to have both CO molecules in a single $\alpha\beta$ dimer (*7*) as a result of the lower free energy of this arrangement (*27*).] Thus it takes 20 μs for the $\alpha_1\beta_2$ interface to lock into place. In Hb_A, the Trpβ37 and Tyrα42 signals develop in concert (*7*), but this is no longer true for Hb_K (Figure 4). The Trpβ37 W3 difference band develops between 1 and 10 μs, while the sigmoidal Y8a/8b bands, which result from upshifted Tyrα42 frequencies (*13*), are only seen after 10 μs.

The Trpβ37···Aspα94 H-bond is at the "hinge" region of the interface, formed by the β_2 C-helix and the α_1 FG corner, while the Tyrα42···Aspβ99 H-bond is at the switch region, formed by the β_2 FG corner and the α_1 C-helix (Figure 2) (*2*). The R−T rearrangement produces reorientation of the "hinge" contacts, and a translation of the "switch" contacts, with altered interdigitation of the side chains. Thus the Aspβ99/Asn substitution not only weakens the H-bond with Tyrα42 but also delays its formation.

The conformational changes that occur in the 20 μs phase also weaken the Fe−His bond in Hb_A (*7*). The stretching mode band maximum is lowered to 215 cm^{-1}, and there is a low-frequency shoulder, reflecting chain heterogeneity (*28*). The band position and shape are the same as in deoxyHb (Figure 3). This is the most direct spectroscopic indication of tension in the T state (*29*). The tension is believed to result from the mechanical stress of F helix displacement parallel to the heme, which is observed in the T crystal structure (*2*). This displacement is apparently in response to the locking-in of the T state contacts in the final phase of the allosteric transition (Figure 1). The motive force may be the formation of the hinge and switch H-bonds, since the FG corner of each subunit is at one of these contacts (Figure 2).

The Fe−His Strain Gauge. The Fe−His bond in deoxyHb_K is highly responsive to pH and IHP (Figure 3). At pH 9 its stretching frequency is at a fully relaxed value (223 cm^{-1}), while at pH 6.5 in the presence of IHP the bond is under as much tension (215 cm^{-1} stretching frequency, with low-frequency shoulder) as in deoxyHb_A. These frequencies are qualitatively in accord with previous visible RR studies of Hb_K (*25, 30, 31*). However, the Fe−His bond is not responsive to pH and IHP in deoxyHb_A (data not shown). It stays tense under all solution conditions. Yet oxygen binding is much more sensitive to allosteric effectors in Hb_A than Hb_k (*10, 11*).

It is evident that the Fe−His stretching frequency cannot be a general purpose monitor of the ligand affinity, as has been proposed (*31*). It is responsive to ligand affinity changes only when the T state contacts are weak. The Fe−His bond is itself rather weak [force constant = ~1 mdyn/Å (*32*)] and is therefore quite sensitive to protein forces. In Hb_K the modest strengthening of the interface contacts which is occasioned by H^+ or IHP binding is sufficient to shift the Fe−His bond from fully relaxed to fully tense. This is the limiting value of the Fe−His bond tension in Hb. The bond cannot be weakened further because there is a limit to how far the F helix can travel within the T quaternary structure. This limit is reached in Hb_A even at pH 9, and further stabilization of the T contacts by H^+ and IHP binding has no additional effect on the Fe−His bond strength, although ligand affinity is strongly decreased. Thus the Fe−His frequency is like a sensitive strain gauge, whose meter is easily pinned. The situation is quite different than envisioned in Hopfield's coupled spring model (*33*), in which the Fe−His bond is represented by a stiff spring and the rest of the protein is represented by a weak spring. In fact, the Fe−His spring is weak, relative to the forces generated via the subunit interfaces, but it is extensible only over a limited range.

CONCLUSIONS

Cooperativity in Hb is controlled by interhelical H-bonds which allow the helices to act as levers, thereby amplifying the motions generated at the heme by ligation and deligation. The levers control the positions of the chain termini that stabilize the T state via intersubunit salt bridges. This picture is consistent with Perutz's original sterochemical hypothesis (*34*), in which changes at the heme were linked to salt-bridge formation, and it clarifies the nature of the links. The allosteric transition is not instantaneous but occurs in a series of steps, well separated in time. The stepwise nature of the process may circumvent a prohibitive activation barrier for the R → T rearrangement, if it had to be carried out in a single step. By providing a pathway with discrete intermediates, each one having a moderate activation energy, the protein increases the probability of a successful quaternary transition.

ACKNOWLEDGMENT

We thank Dr. Franklin Bunn for a generous gift of blood containing Hb Kempsey, Daojing Wang for advice and assistance, and Prof. Shankar Subramanian for helpful discussions.

REFERENCES

1. Perutz, M. (1990) *Mechanisms of Cooperativity and Allosteric Regulation in Proteins*, Cambridge University Press, Cambridge, U.K.
2. Baldwin, J., and Chothia, C. (1979) *J. Mol. Biol. 129*, 175−220.
3. Monod, J., Wyman, J., and Changeux, J.-P. (1965) *J. Mol. Biol. 12*, 88−118.
4. Martin, J. L., Migus, A., Poyart, C., Lecarpentier, Y., Astier, R., and Antonetti, A. (1983) *Proc. Natl. Acad. Sci. U.S.A. 80*, 173−177.
5. Anfinrud, P. A., Han, C., and Hochstrasser, R. M. (1989) *Proc. Natl. Acad. Sci. U.S.A. 86*, 8387−8391.
6. Hofrichter, J., Sommer, J. H., Henry, E. R., and Eaton, W. A. (1983) *Proc. Natl. Acad. Sci. U.S.A. 80*, 2235−2239.
7. Jayaraman, V., Rodgers, K. R., Mukerji, I., and Spiro, T. G. (1995) *Science 269*, 1843−1848.
8. Hildebrandt, P. G., Copeland, R. A., Spiro, T. G., Otlewski, J., Laskowshi, M., and Prendergast, F. G. (1988) *Biochemistry 27*, 5426−5433.

9. Miura, T., Takeuchi, H., and Harada, I. (1989) *J. Raman Spectrosc. 20*, 667−671.
10. Bunn, H. F., Wohl, R. C., Bradley, T. B., Cooley, M., and Gibson, Q. (1974) *J. Biol. Chem. 249*, 7402−7409.
11. Nagai, M., Nishibu, M., Sugita, Y., Yoneyama, Y., Jones, R. T., and Gordon, S. (1975) *J. Biol. Chem. 250*, 3169−3173.
12. Hu, X., and Spiro, T. G. (1997) *Biochemistry 36*, 15701−15712.
13. Rodgers, K. R., Su, C., Subramanian, S., and Spiro, T. G. (1992) *J. Am. Chem. Soc. 114*, 3697−3709.
14. Mukerji, I., and Spiro, T. G. (1994) *Biochemistry 33*, 13132−13139.
15. Turner, G. J., Galacteros, F., Doyle, M. L., Hedlund, B., Pettigrew, D. W., Turner, B. W., Smith, F. R., Moo-Penn, W., Rucknagel, D. L., and Ackers, G. K. (1992) *Proteins 14*, 333−350.
16. Hu, X., Dick, L. A., and Spiro, T. G. (1998) *Biochemistry 37*, 9445−9448.
17. Jayaraman, V., and Spiro, T. G. (1995) *Biochemistry 34*, 4511−4515.
18. Wang, D., and Spiro, T. G. (1998) *Biochemistry 37*, 9940−9951.
19. Kilmartin, J. V., Breen, J. J., Roberts, G. C. K., and Ho, C. (1973) *Proc. Natl. Acad. Sci. U.S.A. 70*, 1246−1249.
20. Jayaraman, V., Rodgers, K. R., Mukerji, I., and Spiro, T. G. (1993) *Biochemistry 32*, 4547−4551.
21. Dasgupta, S., and Spiro, T. G. (1986) *Biochemistry 25*, 5941−5948.
22. Togi, A., Ishimori, K., Unno, M., Konno, T., Morishima, I., Miyazaki, G., and Imai, K. (1993) *Biochemistry 32*, 10165−10169.
23. Lim, M., Jackson, T. A., and Anfinrud, P. A. (1995) *Science 269*, 962−966.
24. Alben, J. O., Beece, D., Bowne, S. F., Doster, W., Einsentein, L., Frauenfelder, H., Good, D., McDonald, J. D., Marden, M. C., Moh, P. P., Reinisch, L., Reynolds, A. H., Shyamsunder, E., and Yue, K. T. (1982) *Proc. Natl. Acad. Sci. U.S.A. 79*, 3744−3748.
25. Scott, T. W., and Friedman, J. M. (1984) *J. Am. Chem. Soc. 106*, 5677−5687.
26. Ackers, G. K., and Johnson, M. L. (1990) *Biophys. Chem. 37*, 265−279.
27. Ackers, G. K., Doyle, M. L., Myers, D., and Daugherty, M. A. (1992) *Science 255*, 54−63.
28. Nagai, K., and Kitagawa, T. (1980) *Proc. Natl. Acad. Sci. U.S.A. 77*, 2033−2037.
29. Nagai, K., Kitagawa, T., and Korimoto, H. (1980) *J. Mol. Biol. 136*, 271−289.
30. Ondrias, M. R., Rousseau, D. L., Shelnutt, J. A., and Simon, S. R. (1982) *Biochemistry 21*, 3428−3437.
31. Matsukawa, S., Mawatari, K., Yoneyama, Y., and Kitagawa, T. (1985) *J. Am. Chem. Soc. 107*, 1108−1113.
32. Kincaid, J., Stein, P., and Spiro, T. G. (1979) *Proc. Natl. Acad. Sci. U.S.A. 76*, 549−552.
33. Hopfield, J. J. (1973) *J. Mol. Biol. 77*, 207−222.
34. Perutz, M. F. (1970) *Nature 228*, 726−734.
35. Shaanan, B. (1983) *J. Mol. Biol. 171*, 31−59.
36. Fermi, G., Perutz, M. F., Shaanan, B., and Fourme, R. (1984) *J. Mol. Biol. 175*, 159−174.

BI982513C